© 2016. Published by The Company of Biologists Ltd | Journal of Cell Science (2016) 129, 1878-1891 doi:10.1242/jcs.182089

RESEARCH ARTICLE

# Cell adhesion molecule L1 contributes to neuronal excitability regulating the function of voltage-gated $Na^+$ channels

**Pierluigi Valente[1], Gabriele Lignani[2,*], Lucian Medrihan[2,‡], Federica Bosco[1], Andrea Contestabile[2], Pellegrino Lippiello[1,§], Enrico Ferrea[2,¶], Melitta Schachner[3], Fabio Benfenati[1,2], Silvia Giovedì[1] and Pietro Baldelli[1,2,**]**

## ABSTRACT

L1 (also known as L1CAM) is a trans-membrane glycoprotein mediating neuron–neuron adhesion through homophilic and heterophilic interactions. Although experimental evidence has implicated L1 in axonal outgrowth, fasciculation and pathfinding, its contribution to voltage-gated $Na^+$ channel function and membrane excitability has remained unknown. Here, we show that firing rate, single cell spiking frequency and $Na^+$ current density are all reduced in hippocampal excitatory neurons from L1-deficient mice both in culture and in slices owing to an overall reduced membrane expression of $Na^+$ channels. Remarkably, normal firing activity was restored when L1 was reintroduced into L1-deficient excitatory neurons, indicating that abnormal firing patterns are not related to developmental abnormalities, but are a direct consequence of L1 deletion. Moreover, L1 deficiency leads to impairment of action potential initiation, most likely due to the loss of the interaction of L1 with ankyrin G that produces the delocalization of $Na^+$ channels at the axonal initial segment. We conclude that L1 contributes to functional expression and localization of $Na^+$ channels to the neuronal plasma membrane, ensuring correct initiation of action potential and normal firing activity.

**KEY WORDS: L1CAM, Sodium channels, Action potential, Firing activity, Adhesion molecule, CRASH syndrome**

## INTRODUCTION

Neural cell adhesion molecule L1 (also known as L1CAM) is a member of the L1 family of structurally related multidomain cell adhesion molecules comprising neuronal-glial cell adhesion molecule (NgCAM), neuronal cell adhesion molecule (NrCAM), neurofascin (NFASC), TAG-1 (also known as CNTN2), close L1 homolog (CHL1) and contactins. These glycoproteins belong to the larger class of immunoglobulin-like cell adhesion molecules that mediate cell-to-cell recognition through $Ca^{2+}$ independent homophilic or heterophilic binding at the cell surface (Kenwrick and Doherty, 1998). L1 is a transmembrane glycoprotein (Lindner et al., 1983) expressed by almost all post-mitotic neurons in the central nervous system (CNS) at the onset of differentiation and by Schwann cells in the peripheral nervous system, but not by glial cells in the CNS (Maness and Schachner, 2007). Evidence for an important role of L1 in development has been obtained from analysis of L1-deficient humans and mice.

Mutations of the L1 gene on Xq28 in humans are responsible for L1 syndrome, formerly known as CRASH syndrome, with patients displaying symptoms such as corpus callosum hypoplasia, mental retardation, adducted thumbs, spastic paraplegia and hydrocephalus (Weller and Gärtner, 2001). A similar phenotype, partially dependent on genetic background, has been described in genetically L1-deficient mice that show hydrocephalus, agenesis of the corpus callosum, abnormal development of the corticospinal tract and other abnormalities affecting distinct neuronal subpopulations (Dahme et al., 1997; Demyanenko et al., 1999). However, this phenotype, first described in C57BL/6 mice, can be substantially attenuated depending on the genetic background of the mouse strain (Guseva et al., 2009). Examination of L1 function *in vitro* has revealed that this adhesion molecule plays important roles in cell adhesion and migration, as well as in axonal outgrowth, fasciculation (Appel et al., 1993; Colombo et al., 2014), pathfinding (Cohen et al., 1998) and myelination (Seilheimer et al., 1989; Wood et al., 1990). Moreover, L1 is important for specifying and regulating synaptic efficacy (Schachner, 1997), synaptogenesis (Enneking et al., 2013), synaptic activity and plasticity (Lüthl et al., 1994), including learning and memory (Law et al., 2003). Finally, L1 is one of the few adhesion molecules known to be beneficial for repair processes in the injured adult CNS of vertebrates owing to its ability to promote axonal re-growth and neuronal survival in rat spinal cord regeneration (Roonprapunt et al., 2003; Becker et al., 2004) and other neurological diseases (Djogo et al., 2013).

Although L1 takes part in many important functional processes in the nervous system (Law et al., 2003; Saghatelyan et al., 2004), whether L1 can affect neuronal membrane excitability is completely unknown. To investigate this issue, we used electrophysiological methods to study the physiology of neurons at network and single cell levels in primary hippocampal cultures and acute slices obtained from L1-deficient mice. We describe for the first time that L1 is crucial for maintaining physiological levels of spontaneous network firing activity. Patch-clamp recordings revealed that genetic deletion of L1 in transgenic mice not only reduces firing activity and $Na^+$ currents at the soma of individual excitatory neurons, but also interferes with the initiation of action potentials at the axon initial segment (AIS). Importantly, these abnormalities could be rescued by re-introduction of full-length L1 into L1-deficient neurons, demonstrating that the observed phenomena are not due to developmental abnormalities, but are

[1]Department of Experimental Medicine, University of Genova, Viale Benedetto XV, 3, Genova 16132, Italy. [2]Center for Synaptic Neuroscience and Technology, Istituto Italiano di Tecnologia, Largo Rosanna Benzi 10, Genova 16132, Italy. [3]Center for Neuroscience, Shantou University Medical College, 22 Xin Ling Road, Shantou, Guangdong 515041, China.
*Present address: Department of Clinical and Experimental Epilepsy, Institute of Neurology, University College London, London WC1N 3BG, UK. ‡Present address: Laboratory of Molecular and Cellular Neuroscience, Rockefeller University, New York, NY, USA. §Present address: Department of Pharmacy, University of Napoli Federico II, Napoli, Italy. ¶Present address: Cognitive Neuroscience, Sensorimotor Laboratory, German Primate Center, Leibniz Institute for Primate Research, Göttingen, Germany.

**Author for correspondence (pietro.baldelli@unige.it)

**Received 19 October 2015; Accepted 8 March 2016**



Journal of Cell Science

Journal of Cell Science (2016) 129, 1878-1891 doi:10.1242/jcs.182089

directly related to L1 function in differentiated neurons. Moreover, this phenotype is not related to a reduction in mRNA levels of voltage-dependent $Na^+$ channels, but to the impaired targeting to the plasma membrane and abnormal localization at the cell surface of $Na^+$ channels. Our data show that L1, apart from controlling axonal growth and migration, plays a new and significant role in the modulation of membrane excitability and neuronal network firing activity.

## RESULTS

### Networks of hippocampal neurons from L1-deficient mice display a reduction in spontaneous firing activity

To investigate the role of L1 in neuronal functions, we first analyzed spontaneous activity of neuronal networks at 18 days *in vitro* (div) after plating hippocampal neurons from wild-type and L1-deficient mice on multielectrode array (MEA) chips (Fig. 1A). As shown by representative extracellular recordings (Fig. 1B) and raster plots of the spiking activity (Fig. 1C), the spontaneous activity of neurons from both wild-type and L1-deficient mice were characterized by the presence of random spikes and action potential bursts. However, L1-deficient networks displayed a lower spiking activity compared to wild-type networks (Fig. 1D). The decrease in the mean spiking rate was due to a reduction of the mean burst rate (Fig. 1E) and of the intra-burst spiking frequency (Fig. 1F), resulting in a reduction of the percentage of spikes occurring during the burst (Fig. 1G). No significant change in burst duration was observed in L1-deficient networks (Fig. 1H). The reduction of burst and intra-burst spiking rates suggests that the lack of L1 impairs the synchronization of the spontaneous activity in the neuronal network.

### Deletion of L1 reduces neuronal intrinsic excitability of excitatory neurons

We next asked whether an altered intrinsic excitability at the level of single excitatory neurons could underlie the differences in the network firing properties observed by MEAs recordings in L1-deficient mice. Excitatory pyramidal neurons were visually identified in low-density hippocampal cultures (Fig. 2A) and analyzed by patch-clamp recordings in current-clamp configuration (Pozzi et al., 2013).

When the membrane potential was persistently depolarized to −40 mV by constant injection of a moderate positive current, wild-type excitatory neurons showed a higher spontaneous firing activity than L1-deficient neurons (Fig. 2B,C). In addition, the firing frequency was studied by delivering constant current pulses (1 s duration) of increasing amplitude (10 pA steps) and measuring the resulting action potential firing rate (Fig. 2D). The analysis of firing rate versus injected current revealed that the L1 deletion significantly reduced the high-frequency firing activity evoked by strongly depolarizing current pulses (Fig. 2E). L1-deficient neurons also showed a marked downregulation of the mean instantaneous firing frequency evoked by a current pulse of 160 pA (Fig. 2F). Moreover, analysis of the shape of the first action potential evoked by minimal current injection (Fig. 2G; typically 60/70 pA, see plot in Fig. 2E) showed that the deletion of

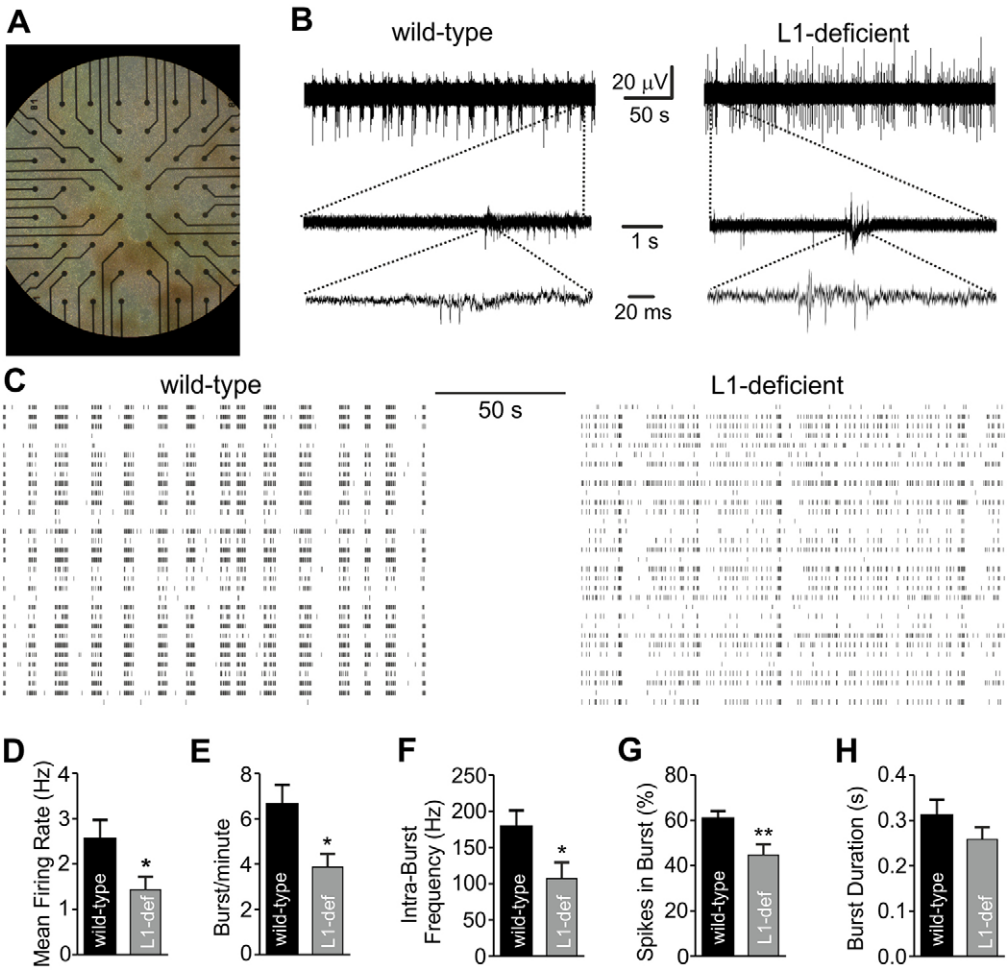


**Fig. 1. Spontaneous activity of the neuronal network is downregulated in the absence of L1.** (A) Representative microphotographs of a wild-type network cultured over a MEA for 18 div (calibration: inter-electrode distance, 200 µm). (B) Representative voltage traces showing the typical firing activity (upper traces) that characterizes wild-type and L1-deficient networks (18 div). Close-ups are of the voltage traces showing burst events (middle traces) and spikes occurring within a burst (lower traces). (C) Raster plots of spontaneous spikes, represented by vertical bars, showing spiking and bursting activities for wild-type (left) and L1-deficient (right) cultures at 18 div. (D–H) Spiking-rate, burst rate, intra-burst frequency, burst duration, intra-burst spiking rate and percentage of spikes in the burst are plotted as means±s.e.m. for both genotypes. **P*<0.05; ***P*<0.01 (unpaired Student's *t*-test; *n*=16 and *n*=12) MEAs from three independent cell preparations from wild-type and L1-deficient mice, respectively.

Journal of Cell Science (2016) 129, 1878-1891 doi:10.1242/jcs.182089

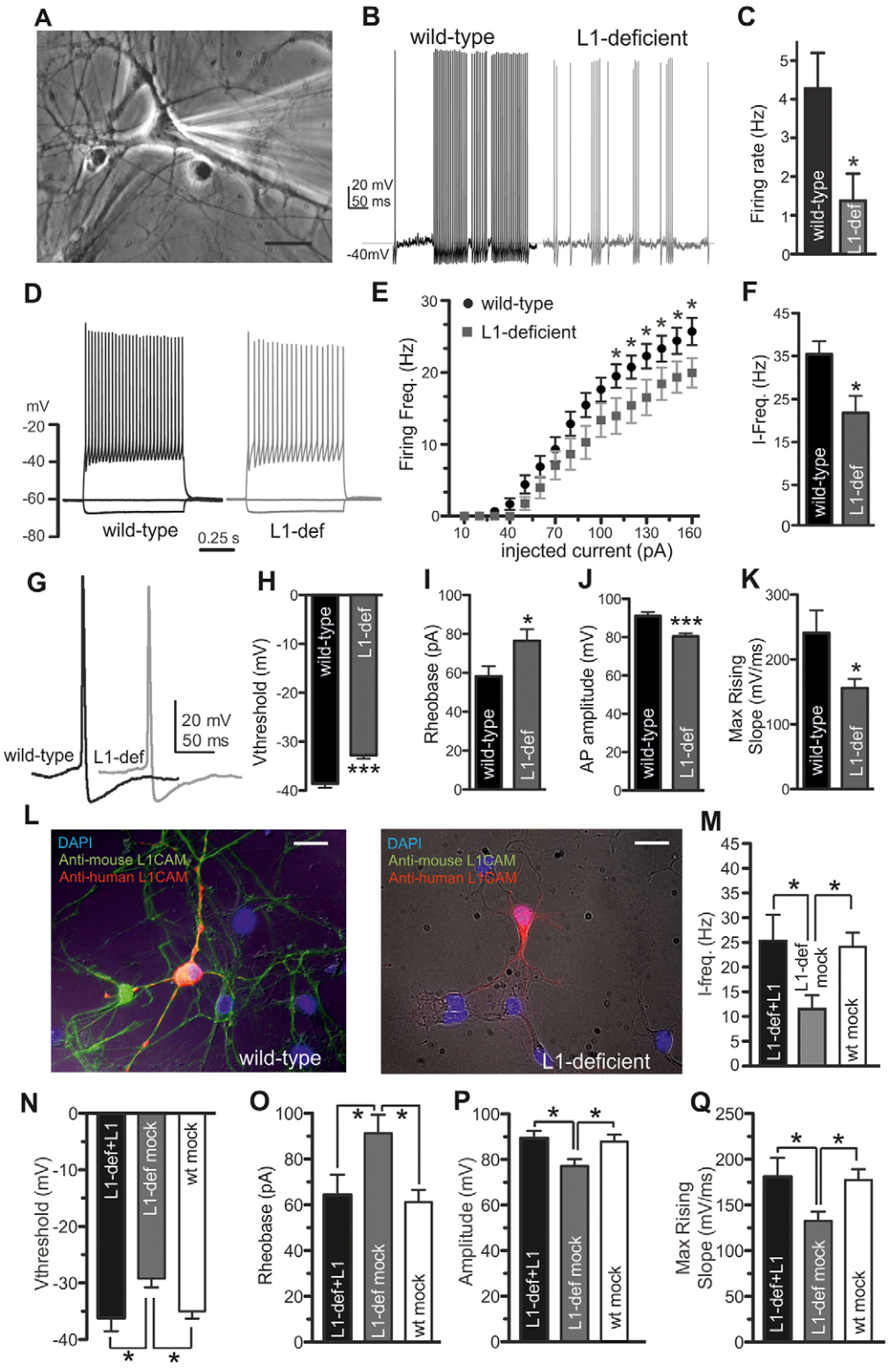


**Fig. 2. Excitability of excitatory neurons is impaired by L1 deletion but its re-expression in L1-deficient neurons rescues their normal firing properties.** (A) Phase-contrast micrograph of representative hippocampal neurons used for current- and voltage-clamp recordings. Scale bar: 20 µm. (B) Representative recordings of spontaneous action potentials induced by injection of a constant depolarizing current that maintains the $V_h$ at –40 mV. (C) Mean±s.e.m. firing rate of spontaneous action potentials in wild-type and L1-deficient neurons. (D) Representative recordings of action potentials induced by the injection of –10, 0 and +100 pA steps for 1 s. (E) Plots of the mean instantaneous firing frequency versus injected current for wild-type (black) and L1-deficient (gray) excitatory neurons. (F) Mean±s.e.m. instantaneous firing-rate calculated in wild-type and L1-deficient excitatory neurons. (G) Representative traces of the shape of the first action potential evoked by minimal current injection recorded in wild-type (black) and L1-deficient (gray) neurons. Bar histograms show mean±s.e.m. voltage threshold (H), rheobase (I), action potential amplitude (J), and maximum rising-slope (K). In C and F–K, *$P$<0.05; ***$P$<0.001 (unpaired Student's $t$-test; $n$=17 for wild-type and L1-deficient neurons). (L) Representative phase-contrast images superimposed onto images obtained by fluorescence microscopy of wild-type (12 div, left) and L1-deficient (12 div, right) neurons transfected with the full-length neuronal isoform of human L1 and immunostained for mouse (green) and human (red) L1. Nuclei are labeled by DAPI. Scale bars: 50 µm. Mean±s.e.m. values of the I-frequency (M), voltage threshold (N), rheobase (O), action potential amplitude (P) and maximum rising-slope (Q), estimated in L1-deficient neurons transfected with L1 (nat-L1; black bars; $n$=9) or with the empty vector (mock; gray bars; $n$=8) and in wild-type neurons transfected with the empty vector (open bars; $n$=9). *$P$<0.05 (one-way ANOVA, followed by the Fisher's test).

L1 shifts the voltage threshold towards more positive values (Fig. 2H), increases the rheobase (Fig. 2I), reduces action potential amplitude (Fig. 2J) and maximum rising slope (Fig. 2K), whereas leaving the other electrophysiological parameters unchanged (Table 1).

The alteration in the firing activity and action potential shape strongly suggest that L1 deletion is causally linked to a change in $Na^+$ channel conductance that primarily defines voltage threshold, rheobase, amplitude and rising slope of the action potential, but also the spiking frequency (Pozzi et al., 2013).

### Expression of the full-length neuronal isoform of L1 in L1-deficient neurons rescues their normal firing properties

The permanent deletion of a protein in constitutive L1-deficient mice could induce functional alterations that might not be directly related to the specific functional role of the protein, but rather to secondary



Journal of Cell Science

Journal of Cell Science (2016) 129, 1878-1891 doi:10.1242/jcs.182089

**Table 1. Electrophysiological parameters describing the passive membrane properties and the shape of the first elicited action potential measured in wild-type and L1-deficient neurons**

| | Wild-type neurons | L1-deficient neurons | *P*-value | Significance |
|---|---|---|---|---|
| Membrane potential (mV) | −51.81±0.929 | −57.54±0.622 | 0.0001 | *** |
| V threshold (mV) | −38.57±0.842 | −32.79±0.661 | 0.0001 | *** |
| Rheobase (pA) | 58.24±5.162 | 76.47±5.937 | 0.027 | * |
| Action potential amplitude (mV) | 91.02±2.05 | 80.40±1.617 | 0.0003 | *** |
| Max rising slope (mV/ms) | 240.8±34.90 | 155.9±14.33 | 0.0315 | * |
| V max (mV) | 52.45±1.637 | 47.59±1.648 | 0.043 | * |
| Firing rate (Hz) | 1.375±0.702 | 2.901±1.238 | 0.0315 | * |
| I-Freq (Hz) | 36.12±2.91 | 23.29±3.73 | 0.0148 | * |
| Width at 0 mV (ms) | 1.656±0.904 | 1.897±0.095 | 0.0772 | ns |
| Afterhyperpolarization (AHP) (mV) | −49.26±1.071 | −46.57±0.998 | 0.0746 | ns |

Results are mean±s.e.m. ($n \geq 17$ for both conditions). *$P$<0.05; ***$P$<0.001, unpaired two-tailed Student's $t$-test. ns, not significant.

compensatory effects occurring during neuronal development. Thus, we evaluated whether the altered firing activity observed in L1-deficient excitatory neurons was specifically and directly related to the lack of L1. To assess this, we determined the capability of the full-length neuronal isoform of human L1, expressed in L1-deficient excitatory neurons, to rescue the normal firing properties observed in wild-type neurons. Hippocampal wild-type and L1-deficient neurons [10 days *in vitro* (div)] were transfected with either human L1 (nat-L1) or the corresponding empty vector (mock) (Fig. 2L). After 76 h, immunostaining with antibodies against mouse and human L1 revealed the presence of both L1 orthologs in wild-type transfected neurons (Fig. 2L, left), whereas L1-deficient neurons were positive only to human L1 (Fig. 2L, right). For patch-clamp experiments, nat-L1 was co-transfected with a tomato fluorescent reporter. Current-clamp recordings revealed that the instantaneous firing frequency (Fig. 2M) and all the parameters describing the action potential shape, such as voltage threshold, rheobase, action potential amplitude and maximum rising slope (Fig. 2N–Q) were rescued to values similar to those observed in wild-type excitatory neurons transfected with the mock vector, indicating that the functional changes induced by L1 deletion are largely reversible.

### Function and expression of $Na^+$ channels are reduced in L1-deficient excitatory neurons

The intrinsic neuronal excitability is tightly dependent on the activity of several types of ion channels. However, the increase in rheobase, the more positive threshold, and the reduction of the action potential maximum rising slope and amplitude (Fig. 2H–K) observed in L1-deficient neurons all strongly suggest an impairment of sodium currents ($I_{Na}$) (Bean, 2007). Thus, we used whole-cell voltage-clamp recordings to evaluate the overall $Na^+$ current density ($I_{Na}$/cell capacitance=$J_{Na}$).

Space-clamp problems affecting $I_{Na}$ recordings in cultured neurons were circumvented by a voltage-step protocol preceded by a brief pre-pulse at −40 mV that inactivates axonal $I_{Na}$ currents, thus allowing isolation of the $I_{Na}$ somatic component (Milescu et al., 2010) (Fig. 3A). Indeed, $I_{Na}$ recorded from cortical pyramidal neurons in slices using such pre-pulse showed a voltage dependence nearly identical to that of $I_{Na}$ recorded from pyramidal neurons lacking axonal and dendritic processes (Milescu et al., 2010). Consistently with the impaired firing activity described above, the $J_{Na}$ evoked at increasing membrane potentials was reduced in the absence of L1 (Fig. 3B). Analysis of the $J_{Na}$ versus voltage (Fig. 3B) revealed that the reduction of $J_{Na}$ in L1-deficient neurons was not associated with any shift in the $J_{Na}/V$ curve. Moreover, the voltage-dependence of the activation (Fig. 3C) and inactivation (Fig. 3D) curves was not affected in the absence of L1, indicating that the reduction of $I_{Na}$ amplitude was not due to a change in the biophysical properties of $Na^+$ channels, but rather to a decrease in the number of functional $Na^+$ channels. To investigate whether the impairment of $J_{Na}$ was accompanied by a downregulation of $Na^+$ channels, we tested the total expression levels of $Na^+$ channels in L1-deficient cells by immunoblotting with an antibody against all $Na^+$ channels. The absence of L1 in cortical neurons determined a significant decrease of $Na^+$ channel protein levels compared to wild-type cultures (Fig. 3E,F, left).

It has been previously shown that L1 mainly interacts with ankyrinB (Boiko et al., 2007), which in turns stabilizes L1 within the axon. Moreover, other members of the L1CAM family of cell adhesion molecules, such as neurofascin and NrCAM, interact with ankyrinG (Bennett and Chen, 2001), which mediates clustering of $Na^+$ channels at the AIS (Zhou et al., 1998; Barry et al., 2014). Thus, it is possible that the effects of L1 deletion can, at least in part, be ascribed to a reduced expression of ankyrinG or ankyrinB. However, immunoblots of L1-deficient cortical neuron cultures did not show any change in the expression level of ankyrinG (Fig. 3F, middle) or ankyrinB (Fig. 3F, right) in comparison to wild-type neurons.

### Deletion of L1 specifically affects the initiation of action potential

An important caveat in the study of $I_{Na}$ and action potential properties by patch-clamp recordings is that these measurements are obtained from the neuronal cell body, although action potentials initiate more distally at the AIS (Stuart et al., 1997; Palmer and Stuart, 2006; Shu et al., 2007; Kole and Stuart, 2008). It has been demonstrated that the membrane potential change rate (i.e. the first derivative d$V$/d$t$) versus voltage, commonly named the phase-plot, exhibits a two-component biphasic increase rate during spike generation. The first component is due to spike initiation in the AIS ('AIS spike') and to its fast antidromic propagation to the soma that generates a sudden voltage increase from baseline called a 'kink' (Shu et al., 2007). The invasion of the soma by the AIS spike generates a delayed activation of $Na^+$ channels in the somatodendritic portions that leads to the second component of phase-plot (the 'somatodenditric spike' or SD spike) (Yu et al., 2008; McCormick et al., 2007) reaching the action potential peak (Fig. 4A–C, upper panels). This phenomenon is observed not only *in vivo,* but also in brain slices and dissociated neurons cultured for

Journal of Cell Science (2016) 129, 1878-1891 doi:10.1242/jcs.182089

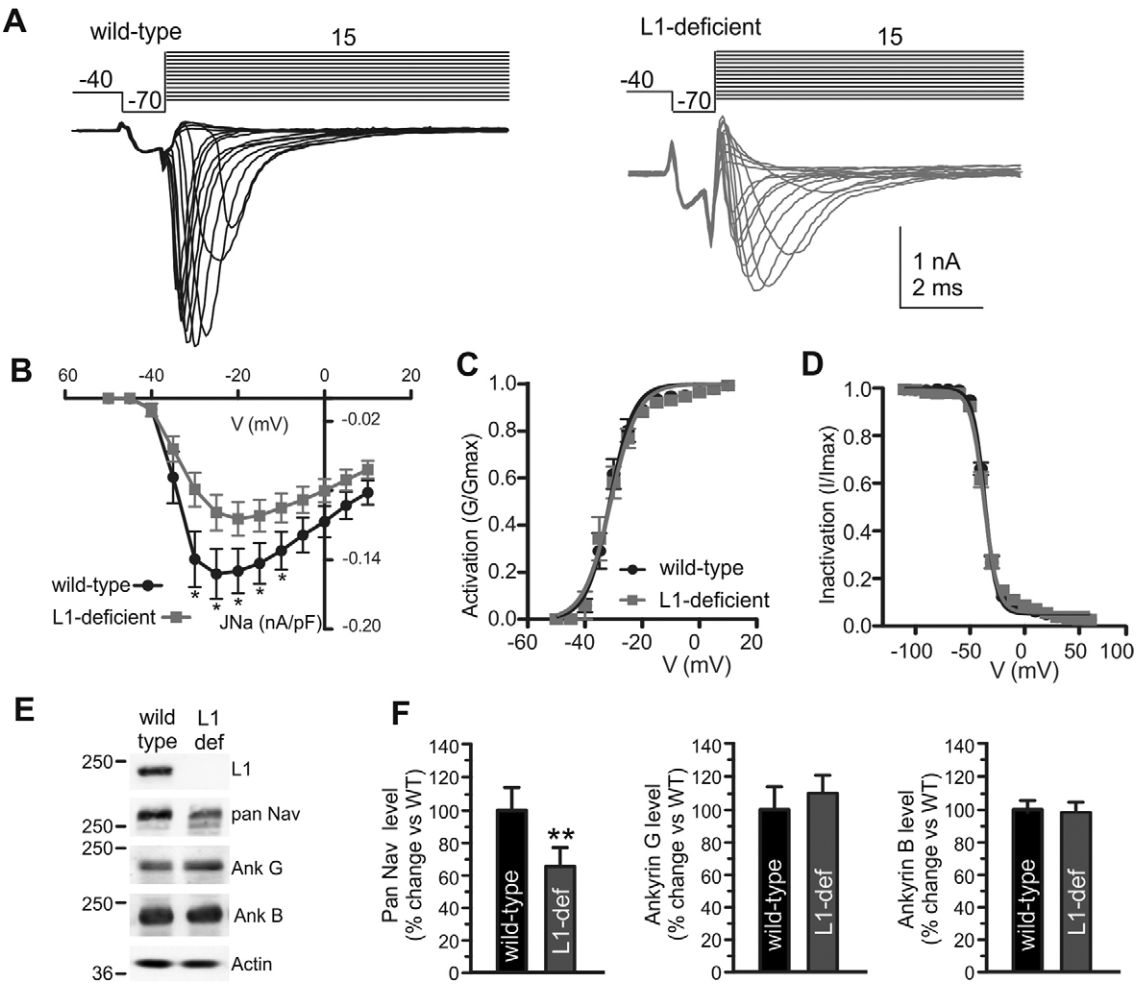


**Fig. 3. The density of voltage-gated sodium currents is downregulated in the absence of L1.** (A). Pre-pulse protocol used and representative somatic $I_{Na}$ current traces recorded in wild-type (black trace) and L1-deficient (gray trace) excitatory neurons. Visually identified excitatory pyramidal neurons were initially clamped at −70 mV and depolarized by a single voltage pre-pulse at −40 mV lasting 5 ms. At 1 ms after the end of the pre-pulse, a series of voltage steps between −60 and +60 mV in 10 mV increments were delivered. (B) Mean±s.e.m. *J–V* relationship for wild-type and L1-deficient excitatory hippocampal neurons calculated using the protocol shown in A. **P*<0.05 (Student's unpaired *t*-test with Welch's correction for non-equal variance; *n*=21 and *n*=24 for wild-type and L1-deficient, respectively). (C) Mean±s.e.m. $G/G_{max}$ relationships (wild-type, *n*=16; L1-deficient, *n*=15) and (D) steady-state voltage dependence of inactivation (wild-type, *n*=27; L1-deficient, *n*=27) were similar in both genotypes. (E) Representative immunoblots of lysates of cultured cortical neurons (after 14 div) obtained from wild-type and L1-deficient mice using antibodies against L1, $PanNa_v$, ankyrinG, ankyrinB and actin. Actin immunoreactivity was used as loading control. Molecular masses are shown on the left in kDa. (F) Bar plots of the mean±s.e.m. immunoreactive levels of Pan-Nav (left), ankyrinG (middle) and ankyrinB (right) in wild-type and L1-deficient neurons, respectively. ***P*<0.01 (unpaired Student's *t*-test; *n*=6 independent pairs of samples).

more than 2 weeks. In contrast, the kink is absent in acutely dissociated neurons in which action potential recordings are performed a few hours after cellular dissociation (Bean, 2007).

To investigate in more detail the role of L1 in action potential initiation at the AIS, we examined the onset kinetics of somatically recorded action potentials. The shape of the averaged action potential (Fig. 4A) evoked by constant current injection that maintains the holding voltage ($V_h$) at −40 mV (see Fig. 2B) was analyzed by using the plot of the time derivative of voltage ($dV/dt$) versus time (Fig. 4B) and versus voltage (Fig. 4C), allowing a better resolution of the fast change in kinetics of action potential initiation that depends on $Na^+$ channel conductance. Phase-plots graphs of the membrane potential slope ($dV/dt$) versus membrane potential showed strong differences between wild-type and L1-deficient pyramidal neurons (Fig. 4C, upper and lower panels, respectively). Interestingly, the averaged phase-plots revealed that the 'kink' was virtually lost in L1-deficient neurons (Fig. 4D,E). To quantify such differences, we measured the slope of the phase-plot at a *y*-axis value of 4 mV $ms^{-1}$ (Fig. 4F). Such a parameter, termed a 'phase-slope', has been used to measure the steepness of action potentials at their onset (Naundorf et al., 2006; McCormick et al., 2007). The phase-slope was, in fact, significantly reduced in the absence of L1 (Fig. 4F).

Collectively, these results suggest that absence of L1 reduces the intrinsic excitability of isolated excitatory neurons by affecting voltage-gated channels expressed not only in the cell soma, but also at the AIS.

### Alterations of neuronal excitability are conserved in mature CA1 pyramidal neurons of acute hippocampal slices

The data collected in cultured hippocampal excitatory neurons revealed that the absence of L1 affects neuronal firing activity due to a defect in $I_{Na}$. To evaluate whether such a defect is still present in L1-deficient neurons in the intact brain of young mice [postnatal day (P)21–24], we compared neuronal firing properties in CA1 pyramidal neurons in acute hippocampal slices (Fig. 5A).

Journal of Cell Science (2016) 129, 1878-1891 doi:10.1242/jcs.182089

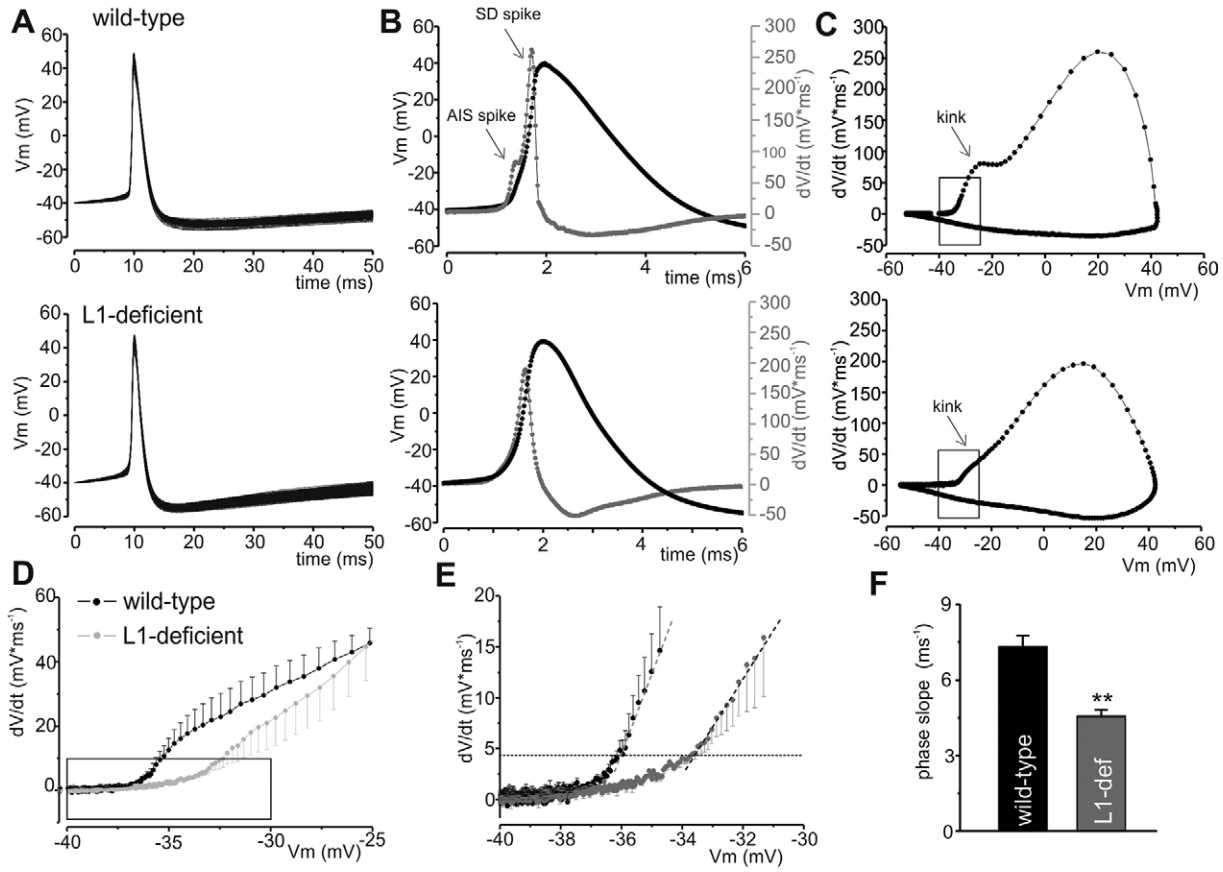


**Fig. 4. Kinetics of action potential initiation in wild-type and L1-deficient excitatory neurons.** (A) Overlay of representative action potentials recorded in wild-type (upper panel) and L1-deficient (lower panel) neurons. Action potentials were activated by the delivery of a persistent depolarizing current that maintains the $V_h$ a few mV above threshold. (B) Average of the action potentials shown in A, superimposed onto the time course of the first derivative of the averaged membrane voltage (d*V*/d*t*) in wild-type (upper panel) and L1-deficient (lower panel) neurons. The arrow shows the characteristic kink at action potential onset (AIS spike), detectable only in the wild-type neuron. SD, somato-dendritic. (C) Representative plots of the first derivative of the membrane voltage (d*V*/d*t*) versus membrane voltage ($V_m$) (phase-plots) for wild-type (upper panel) and L1-deficient (lower panel) neurons. Note that only wild-type neurons (upper panel) show two clear components in the (d*V*/d*t*) versus ($V_m$) plot, with the AIS component causing the kink followed by the delayed SD component (upper panel). Note the almost complete disappearance of the AIS component and the smoothly rising d*V*/d*t* in the L1-deficient neuron (lower panel). (D) Averaged (d*V*/d*t*) versus ($V_m$) in the range between −40 and −25 mV to highlight the difference in the rate of rise action potential initiation (kink) between wild-type and L1-deficient neurons ($n$=6 for each genotype). (E) Close-up of the averaged phase-plot of D, showing the rapid spike initiation and linear regression fit used to calculate the phase slope. (F) Mean±s.e.m. phase-slope measured at 4 mV/ms in wild-type and L1-deficient neurons **$P$<0.05 (unpaired Student's $t$-test; $n$=6 for each genotype).

Spontaneous firing activity was evoked in CA1 pyramidal neurons through injection of a constant depolarizing current that brought the $V_h$ to −50 mV (Fig. 5B). Under this condition, the mean firing frequency reached by the L1-deficient neurons was 50% lower than that of wild-type neurons (Fig. 5C).

To better appreciate changes in the dynamics of action potential initiation, the shape of the single action potential evoked by current injection was analyzed using the plot of the time derivative of voltage (d*V*/d*t*) versus membrane voltage ($V_m$) (Fig. 5D). As observed in cultured excitatory neurons, the absence of L1 reduced the action potential kink in CA1 neurons of hippocampal slices (Fig. 5D). The change of the kink was quantified by a linear regression fit of the eight experimental points that follow the threshold, set at 4 mV/ms (Fig. 5E) and the corresponding slope (the phase-slope), was significantly reduced in L1-deficient neurons (Fig. 5F). We also investigated the $Na^+$ channel expression levels in cortices of 21-day-old L1-deficient mice relative to wild-type mice by immunoblotting (Fig. 5G). Similar to the results obtained in primary cultures, the absence of L1 induced a decrease in $Na^+$ channel protein levels (Fig. 5H, left), leaving unchanged the levels of ankyrinG (Fig. 5H, middle) and ankyrinB (Fig. 5H, right).

### Absence of L1 induces a distal relocalization of AIS

Previous reports have established that L1 is involved in axonal outgrowth (Appel et al., 1993). When we measured the axonal length in cultured cortical neurons at early stages of neuronal development (2 and 4 div) by immunostaining for the axonal marker SMI-312 (Chung et al., 2003) (Fig. 6A), we found that axon outgrowth was significantly impaired at both time points in the absence of L1 (Fig. 6B).

The strong functional impairment of neuronal excitability and the alteration of the kink that are related to AIS modification, suggested that the absence of L1 could alter the localization of $Na^+$ channels in this subcellular compartment. It is known that $Na^+$ channels are localized at the AIS through interactions with the scaffolding protein ankyrinG (Garrido et al., 2003; Pan et al., 2006) and accumulation of $Na^+$ channels in the AIS makes it the lowest threshold site for action potential initiation (Kole and Stuart, 2008). Thus, we asked whether the impaired axonal elongation at early stages of *in vitro*

Journal of Cell Science (2016) 129, 1878-1891 doi:10.1242/jcs.182089

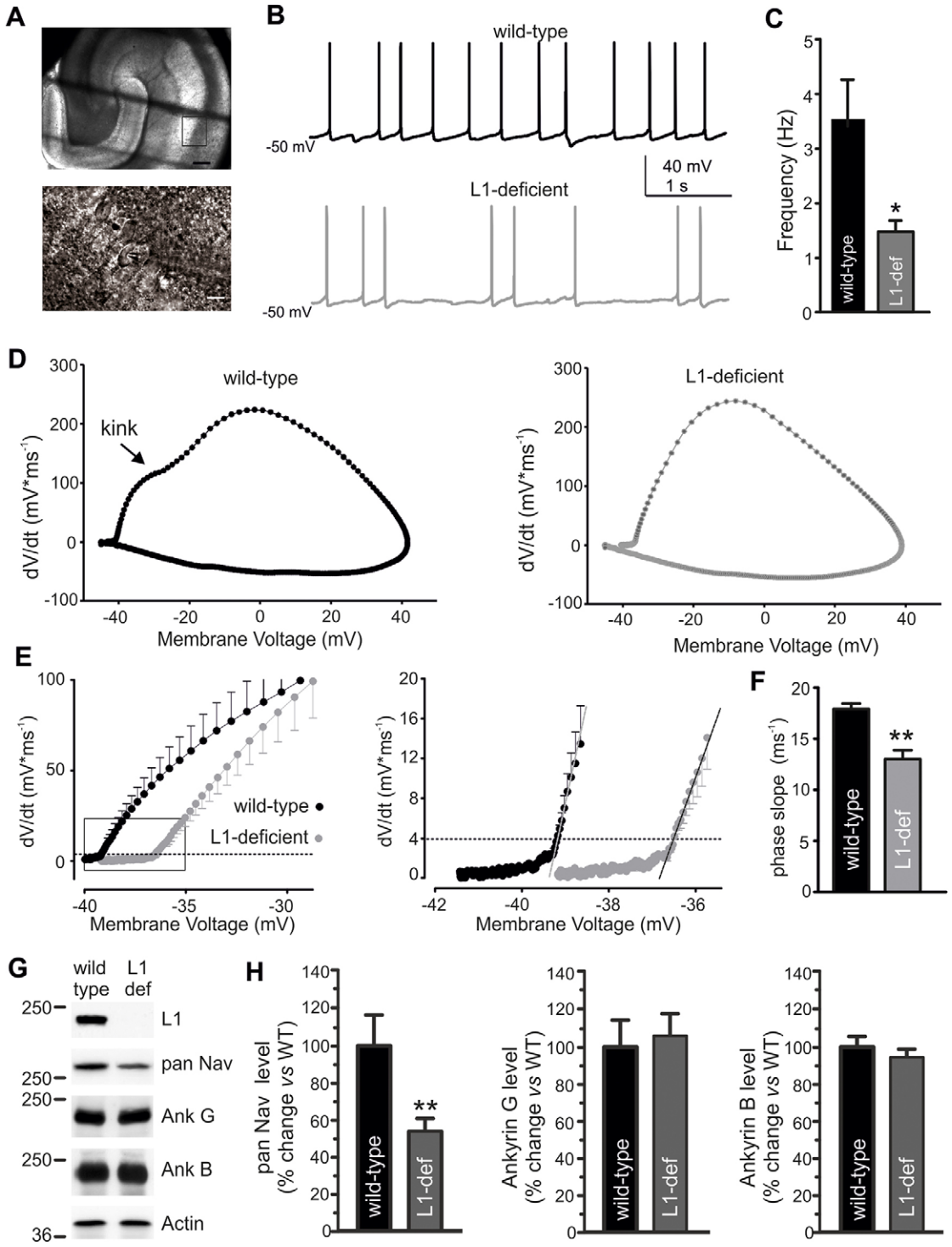


**Fig. 5. Reduction of the firing frequency and suppression of the action potential kink in CA1 pyramidal neurons from L1-deficient acute hippocampal slices.** (A) Representative pictures of an acute hippocampal slice (upper panel) obtained from a (P30) wild-type mice and close-up (lower panel) of a patched CA1 pyramidal neuron. Scale bar: 300 µm (upper panel); 10 µm (lower panel). (B) Voltage traces recorded in CA1 pyramidal hippocampal neurons ($V_h$=−50 mV) from acute slices of wild-type (black) and L1-deficient (gray) mice. (C) Mean±s.e.m. firing frequency in wild-type ($n$=12; black) and L1-deficient ($n$=13; gray) mice. *$P$<0.05 (unpaired Student's $t$-test). (D) Representative plots of the first derivative of the membrane voltage (d$V$/d$t$) versus ($V_m$) (phase-plots) for wild-type (black, left) and L1-deficient (gray, right) CA1 pyramidal neurons. The arrow indicates the action potential kink clearly evident in the wild-type neuron and absent from the L1-deficient neuron. (E) Left: close-up of the mean±s.e.m. phase-plots of wild-type (black) and L1-deficient (gray) neurons. Right: close-up of the mean±s.e.m. phase-plot, showing the rapid spike initiation and the linear regression fit used to calculate the phase slope. (F) Mean±s.e.m. phase slope for wild-type (black) and L1-deficient (gray) estimated by the linear regression of the first 11 points with a d$V$/d$t$>4 mV/ms (see E). **$P$<0.01 (unpaired Student's $t$-test; $n$=9 neurons for wild-type and $n$=10 L1-deficient neurons; three mice per genotype were used). (G) Representative immunoblots of post-nuclear supernatant fractions from P21 wild-type and L1-deficient cortices with antibodies against L1, PanNa$_v$, ankyrinG, ankyrinB and actin. Actin immunoreactivity was used to control for equal loading. Molecular masses are shown on the left in kDa. (H) Mean±s.e.m. immunoreactive levels of PanNa$_v$ (left panel), ankyrinG (middle panel) and ankyrinB (right panel) in wild-type and L1-deficient mice, respectively. **$P$<0.01 (unpaired Student's $t$-test $n$=6 independent pairs of samples).

Journal of Cell Science (2016) 129, 1878-1891 doi:10.1242/jcs.182089

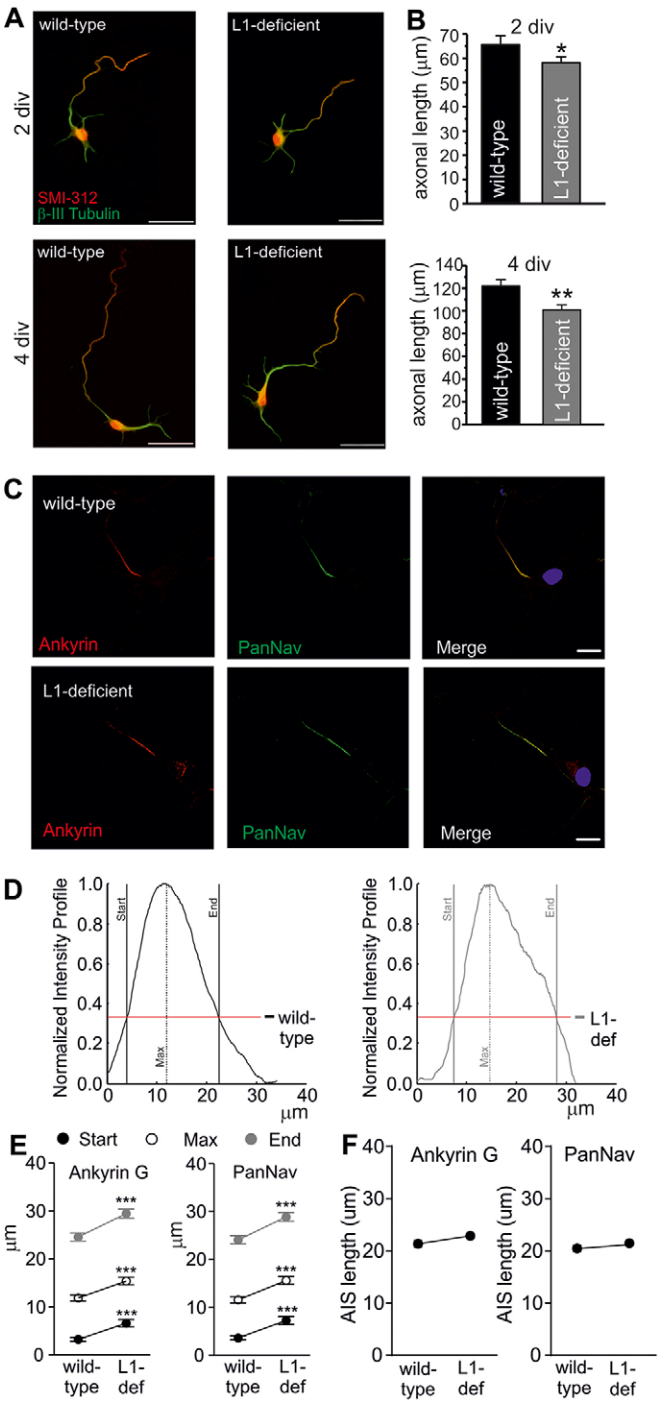


**Fig. 6. Deletion of L1 moves the AIS away from the soma.**
(A) Representative merged images of wild-type and L1-deficient cortical neurons fixed at 2 and 4 div and stained for β-III tubulin (green) and SMI-312 (red). Axonal elongation was measured using ImageJ, based on SMI-312 staining. Scale bars: 40 µm. (B) Mean±s.e.m. axonal length from wild-type ($n$=100) and L1-deficient ($n$=100) neurons from $n$=6 independent experiments; *$P$<0.05; **$P$<0.01 (unpaired Student's $t$-test). (C) Representative images of wild-type and L1-deficient cortical neurons stained at 14 div with ankyrinG (red) and PanNa$_v$ (green) antibodies to evaluate the AIS. Scale bars: 10 µm. (D) Fluorescence intensity profile of ankyrinG signal along the axon of wild-type (left) and L1-deficient (right) cortical neurons fixed at 14 div. Red lines represent the threshold value of fluorescence intensity, used to define start and end of the AIS (33% of the maximum fluorescence intensity). (E) Comparative analysis of the mean±s.e.m. distance from the cell body of the start, maximum and end of AIS, respectively, identified by ankyrinG (left) and PanNa$_v$ (right) immunostaining in wild-type and L1-deficient cortical neurons. ***$P$<0.001 (Mann–Whitney U-test; 14 div neurons, $n$=13 and $n$=14 coverslips for wild-type and L1-deficient, respectively, from $n$=4 independent experiments). (F) Mean±s.e.m. AIS length evaluated by ankyrinG (left) and PanNa$_v$ (right) immunoreactivities. No significant difference for wild-type compared to L1-deficient neurons (Mann–Whitney U-test; $n$=75 and $n$=80 for wild-type and L1-deficient, respectively, from four independent experiments).

development (2–4 div) was associated with an altered organization of AIS in more mature neurons. To assess this, we analyzed the length and location of the AIS in cultured cortical neurons (14 div) by confocal microscopy (Fig. 6C).

Immunostaining for the AIS scaffolding protein ankyrinG showed that start, maximum and end of the AIS were shifted away from the soma in L1-deficient neurons (Fig. 6C–E), whereas the AIS length was unaffected (Fig. 6F, left). This effect was associated with a distal shift of $Na^+$ channels stained by a pan-$Na^+$ channel antibody in L1-deficient neurons (Fig. 6C–F). The absence of L1 relocated both ankyrinG and $Na^+$ channels up to 8 µm away from the soma. This finding is particularly interesting, as it has been demonstrated that the AIS position positively correlates with threshold current density (Grubb and Burrone, 2010). Therefore, the relocation of the AIS is consistent with the more positive voltage threshold and the higher rheobase is found in L1-deficient neurons.

### Impaired membrane targeting of $Na^+$ channels at the plasma membrane of L1-deficient neurons

The reduction in $Na^+$ channel levels observed in L1-deficient lysates from cultured cortical neurons (Fig. 3E,F) and homogenates of cerebral cortices (Fig. 5G,H) could be related to L1-dependent effects on $Na^+$ channel transcription. Indeed, it has been demonstrated that L1 undergoes proteolytic processing by various enzymes, including γ-secretase, which results in translocation of these fragments to the nucleus where they can modulate the transcription of genes (Lutz et al., 2012; Cavallaro and Dejana, 2011). In addition, L1 activates ERK1 and ERK2 (ERK1/2, also known as MAPK3 and MAPK1) signaling (Schaefer et al., 1999; Silletti et al., 2004), which could possibly affect transcription of genes coding for the Na$_v$ α-subunits (Yanagita et al., 2003).

To evaluate whether the effects of L1 deletion on neuronal excitability are attributable to ERK1/2 activation, we quantified the levels of phosphorylated (P)-ERK in homogenates from cerebral cortices of 18- to 21-day-old mice by immunoblotting with phosphorylation-specific antibodies (Fig. 7A). No changes in phosphorylation of ERK1/2 were detected in L1-deficient versus wild-type lysates. Likewise, no changes in the levels of Na$_v$1.1, 1.2 or 1.6 (*SCN1A*, *SCN2A* and *SCN8A*) mRNAs, representing the three main α1 subunits in developing and mature neurons (Vacher et al., 2008) and of ankyrinG mRNA were observed by quantitative PCR (Fig. 7B). The combined data indicate that the reduced levels of $Na^+$ channels in L1-deficient mice are not due to reduced transcription, but could be ascribed to an effect of L1 on $Na^+$ channel trafficking and/or stability.

To investigate this possibility, surface biotinylation assays were performed on live primary cortical neurons. Interestingly, the reduced levels of $Na^+$ channels observed in total lysates of L1-deficient neurons (Fig. 7C; see also Fig. 3F) were fully attributable to a decrease in the biotinylated fraction corresponding to $Na^+$ channels exposed at the cell surface (Fig. 7C,E), whereas the levels of $Na^+$ channels in the intracellular fraction were not changed (Fig. 7C,D). These results demonstrate that the reduction of $Na^+$ channels in L1-deficient neurons is accompanied by their impaired

Journal of Cell Science (2016) 129, 1878-1891 doi:10.1242/jcs.182089

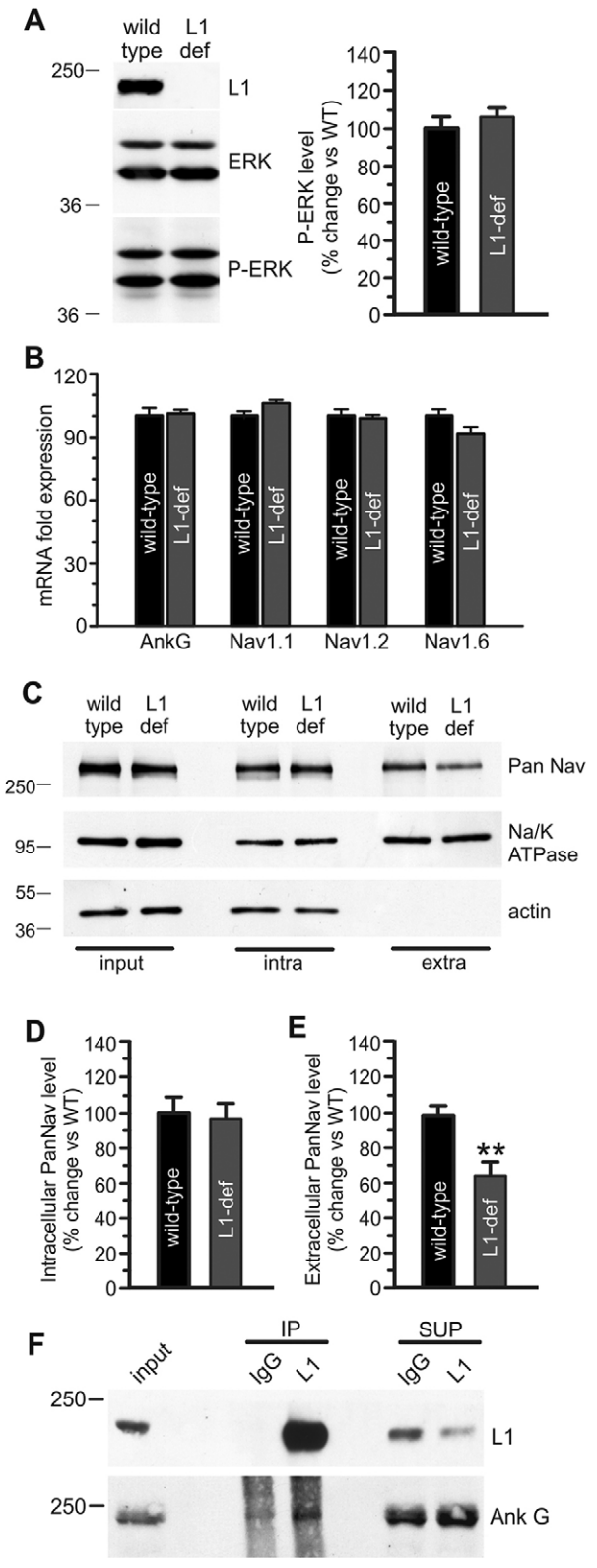


**Fig. 7. Deletion of L1 impairs trafficking of $Na^+$ channels to the plasma membrane.** (A) Representative blots (left panel) and bar plot (right panel; mean±s.e.m.) of the levels of phosphorylated (P-)ERK1/2 in post-nuclear supernatant fractions from P18 wild-type and L1-deficient cerebral cortices with total and active ERK1/2 (P-ERK) antibodies ($n$=6 independent pairs of samples). (B) Bar plot showing quantitative PCR analysis (means±s.e.m.) of ankyrinG, $Na_v1.1$, $Na_v1.2$ and $Na_v1.6$ mRNA transcript levels in wild-type and L1-deficient cerebral cortices obtained from P18 wild-type and L1-deficient mice ($n$=6 independent pairs of samples). (C) Representative immunoblots of cell surface biotinylation experiments performed on wild-type and L1-deficient cortical neurons at 14 div. Equal amounts of total lysate (input), non-biotinylated (intracellular) and biotinylated (extracellular) fractions were assessed by immunoblotting for the $PanNa_v$, Na/K ATPase and actin antibodies. Molecular masses are shown on the left in kDa. Actin and Na/K ATPase immunoreactivities were used as markers of biotin leakiness and equal loading, respectively. (D) Intracellular and (E) cell surface $PanNa_v$ immunoreactivity in L1-deficient neurons is expressed in percent of the respective wild-type levels after normalization of the bands to Na/K ATPase immunoreactivity (mean±s.e.m.). **$P$<0.01 (unpaired Student's $t$-test; $n$=3 independent experiments). (F) Co-immunoprecipitation of ankyrinG with L1. Detergent extracts of mouse brain were immunoprecipitated with goat antibodies specific for L1 or with the respective control goat IgGs, as indicated (IP). The immune complexes together with aliquots of the starting material (input) and of the supernatants (SUP) were subjected to immunoblotting using antibodies against L1, to test the immunoprecipitation efficiency, and against ankyrinG. An immunoblot representative of $n$=3 independent experiments is shown.

targeting to the neuronal plasma membrane that can be due to the loss of a direct or indirect interaction with L1.

Immunoprecipitation assays from mouse brain extracts with anti-L1 antibodies showed that L1, similarly to other L1CAMs proteins (Bennett and Baines, 2001), interacts with ankyrinG (Fig. 7F). Considering that the interaction of ankyrinG with $Na^+$ channels was extensively described (Garrido et al., 2003), our results indicate that an indirect interaction of L1 with $Na^+$ channels could occur, mediated by their binding to ankyrinG scaffold.

## DISCUSSION

The gene encoding L1 is located on the X chromosome (Xq28) (Djabali et al., 1990). More than 200 mutations in this gene (http://www.l1cammutationdatabase.info), underlie a wide spectrum of nervous system abnormalities, collectively named L1 syndrome, including X-linked hydrocephalus (XLH) (Van Camp et al., 1993) and the MASA (mental retardation, aphasia, shuffling gait and adducted thumbs) syndrome (Boyd et al., 1993) in addition to X-linked spastic paraplegia (Kenwrick et al., 1986). Patients bearing nonsense mutations in the L1 extracellular domain express only 10% of the totally synthesized L1 glycoprotein in the plasma membrane and are mentally disabled with an IQ of less than 50 (Kamiguchi et al., 1998). Abnormal neuronal excitability is characteristic of several syndromes associated with cognitive deficits, such as fragile-X syndrome, Rett syndrome and autism spectrum disorders (Shepherd and Katz, 2011; Huber et al., 2002; Fassio et al., 2011), calling for a characterization of the role of L1 in maintaining the physiological neuronal network activity.

In the present study, we have shown a key role for L1 in keeping normal levels of firing activity in hippocampal neuronal networks *in vitro*. The absence of L1 not only reduced the mean firing frequency, but also desynchronized the spontaneous network activity pattern. It has been shown that L1 is involved in neuronal migration, axonal outgrowth and fasciculation, as well as synaptogenesis and synaptic plasticity (Lindner et al., 1983; Kunz et al., 1996; Appel et al., 1993; Dityatev et al., 2010; Dityatev and Schachner, 2003). However, network activity is essential for the refinement of network connections that is based on the spontaneous electrical activity of developing neurons as a requirement for the correct early axon pathfinding decisions (Goulding, 2004).

A reduction in network excitability could be associated with either impairments of the inhibitory–excitatory balance or dysfunctions in ion channel conductance. The spectrum of the action potential parameters altered by L1 deletion observed in both cultured neurons

Journal of Cell Science (2016) 129, 1878-1891 doi:10.1242/jcs.182089

and CA1 neurons of hippocampal slices, including a decrease in the firing rate and alterations of voltage threshold, rheobase, action potential amplitude and maximum rising slope, strongly indicate a defect in $Na^+$ channel function. Indeed, the observed decrease in the somatic $I_{Na}$ density was paralleled by a decrease in the cell surface expression of $Na^+$ channels. This abnormality was largely rescued by reintroduction of the full-length neuronal isoform of L1, demonstrating that the functional changes are direct effects of L1 deletion and do not reflect secondary compensatory changes during development.

It has been shown that the highest density of $Na^+$ channels expressed by a neuron is present at the AIS (Kole et al., 2008) and that action potentials recorded in brain slices and long-term primary cultures, but not in acutely dissociated neurons, are characterized by a rapid ('kinky') onset (Bean, 2007). This feature, owing to the initiation of action potential at the AIS, followed by its back-propagation to the somatodendritic compartment, results in an unusually high rate of rise of membrane potential at the foot of the action potential recorded in the soma (Yu et al., 2008). By using the sensitive phase-plot analysis of the action potential shape, we demonstrate that L1 deletion also affects action potential initiation at the AIS. Indeed, the deletion of L1 produced virtually 'kinkless' action potentials in both dissociated excitatory neurons and CA1 pyramidal neurons in acute slices. This effect was paralleled by a distal relocation of the AIS that moved the AIS components ankyrinG and the $Na^+$ channels a considerable distance away from the soma.

Shifts and changes in length of the AIS have recently been associated with homeostatic responses of neurons that vary their intrinsic excitability in response to sustained lack or increase in activity (Kuba et al., 2010; Grubb and Burrone, 2010). In chronically depolarized primary hippocampal cultures (Grubb and Burrone, 2010), a condition that induced a net decrease of firing activity, $I_{Na}$ and $Na^+$ channel expression levels (Pozzi et al., 2013), AIS relocation has been reported, similar to what we found in L1-deficient neurons. In agreement with our results, the higher distance of the AIS from the soma correlated with a higher rheobase (i.e. current threshold density) and a lower firing frequency. This result indicates that variation in the position of the AIS with respect of the soma is an important source for modulation of spike threshold, rheobase and firing rate, and that L1 is a key determinant of AIS assembly and localization. However, the loss of L1 also impairs the action potential amplitude and maximum rising slope, effects that cannot be easily explained by AIS relocation. These effects are likely to reflect the reduced membrane expression of $Na^+$ channels in L1-deficient neurons, functionally observed by measurement of somatic $Na^+$ current density and biochemically confirmed by immunoblot analysis in cultured primary neurons and slices of adult hippocampus.

How can L1 control membrane expression of $Na^+$ channels? One possible mechanism is by acting as a transcriptional modulator (Cavallaro and Dejana, 2011). Indeed, it has been shown that upon ectodomain shedding, L1 undergoes intramembrane processing by γ-secretase, resulting in the release of a soluble intracellular domain that enters the nucleus and modulates genes transcription (Riedle et al., 2009). Moreover, L1 enhances the expression of MAP2a, MAP2b and MAP2c in cultured hippocampal neurons through the activation of the ERK1/2 pathway (Poplawsky and Dierolf, 2012) and ectopic L1 expression in cell lines induces sustained activation of ERK1/2 with concomitant induction of ERK-regulated gene products (Silletti et al., 2004). The latter report is particularly interesting, as it has been recently shown that ERK1/2 activation affects the stability of mRNA encoding $Na_v1.7$ in bovine adrenal chromaffin cells, resulting in a decreased cell surface expression of functional $Na^+$ channels (Yanagita et al., 2003). However, our results showed that loss of L1 does not affect the ERK activation state or the levels of mRNAs encoding the three main α1 subunits, $Na_v1.1$, 1.2 and 1.6, expressed in hippocampal neurons (Vacher et al., 2008).

Thus, we considered the possibility that the deletion of L1 influences the trafficking or the stability of $Na^+$ channels at the neuronal plasma membrane. Indeed, surface biotinylation analysis revealed that the reduction of $Na^+$ channel protein observed in L1-deficient neurons is mainly due to an impaired targeting of $Na^+$ channels to the cell surface plasma membrane. Although the molecular mechanism underlying this effect has not been investigated in detail, we observed that L1 also associates with ankyrinG, similar to neurofascin and NrCAM, which reversibly bind ankyrinG through their cytoplasmic domain (Davis and Bennett, 1994; Bennett and Baines, 2001; Hortsch et al., 2009; Nishimura et al., 2003). Previous reports have extensively shown a direct interaction of ankyrinG with $Na^+$ channels through an ankyrin-binding domain found in the intracellular loop II–III of $Na_v1.1$, 1.2 and 1.6 subunits (Garrido et al., 2003; Gasser et al., 2012; Lemaillet et al., 2003). Considering that ankyrinG is specifically localized at the AIS and nodes of Ranvier (Rasband, 2008), these results suggest that in the absence of L1 the precise localization of ankyrinG and $Na^+$ channels at the AIS is altered.

At the soma and dendrites, L1 and $Na^+$ channels likely interact through their concomitant binding to distinct scaffold proteins, such as ankyrinB. Indeed, it has been previously shown that ankyrinB and L1 are more widely expressed along the entire length of axons and in the perisomatic region (Boiko et al., 2007) and that L1 interacts with ankyrinB (Chan et al., 1993; Nishimura et al., 2003; Boiko et al., 2007). Moreover, ankyrinB-deficient mice exhibit a phenotype similar to, but more severe than, L1-deficient mice, and share features of human patients bearing L1 mutations (Scotland et al., 1998). Considering that $Na^+$ channels are concentrated, but not exclusively expressed (Colbert and Johnston, 1996), at the AIS (Kole et al., 2008) and nodes (Rasband, 2008), it is plausible to speculate that an L1-dependent enhancement of the binding of $Na^+$ channels to ankyrinB might favor $Na^+$ channels expression at the whole neuronal plasma membrane. This view is in agreement with our observations that L1 deletion not only affects $Na^+$ channel function and localization at the AIS, but also action potential firing properties and $Na^+$ current density at the soma of excitatory neurons without altering ankyrinB or ankyrinG expression levels.

Another possible mechanism to explain the impaired function and translocation of $Na^+$ channels to the plasma membrane is suggested by high structural similarity of L1 with $Na^+$ channel accessory β-subunits (Isom and Catterall, 1996). These subunits play a fundamental role in directing the expression of $Na^+$ channels to the cell surface by organizing the intracellular cytoskeleton through ankyrin- and spectrin-mediated interactions (Isom, 2002; Malhotra et al., 2002). Along with these considerations, it is possible that L1 exerts a function similar to that played by the β-subunits or, alternatively, that the interactions of β-subunits with extracellular matrix components, transmembrane adhesion molecules and intracellular cytoskeletal or signaling proteins are impaired in the absence of L1, resulting in a defective localization and stabilization of $Na^+$ channels at the plasma membrane.

In conclusion, we uncovered a new role of L1 in the targeting of $Na^+$ channels to the neuronal plasma membrane, thereby allowing

Journal of Cell Science (2016) 129, 1878-1891 doi:10.1242/jcs.182089

their physiologically correct functional integration. The data indicate that L1 is crucial to assure functional expression of $Na^+$ channels through interactions with ankyrins and/or other as yet unknown linker proteins. Altered neuronal excitability caused by L1 deletion results in a downgrading of the electrical properties of neurons that underlie the reliability of information transfer in neurons, and hence neural network activity. These findings might thereby offer a mechanistic explanation for the cognitive impairments associated with L1 mutations in humans.

## MATERIALS AND METHODS

### Animals

Constitutively L1-deficient mice are as described previously (Rolf et al., 2001). Given that the L1 gene is located on the X chromosome, L1-deficient males were obtained by mating wild-type males on the 129SvJ/NMRI background with heterozygous females on the 129SvJ/NMRI background. Mice were genotyped by PCR. All experiments were carried out in accordance with the guidelines established by the European Communities Council (Directive 2010/63/EU of September 22nd, 2010) and approved by the Italian Ministry of Health.

### Primary cultures of dissociated hippocampal and cortical neurons

Cultures from hippocampus and cerebral cortex were prepared from 0- to 1-day-old wild-type and L1-deficient mice, as previously described (Beaudoin et al., 2012; Dityatev et al., 2000). Gain-of-function analysis was performed by transfection of the full-length neuronal isoform of L1 into L1-deficient neurons transfected with 1 µg of DNA encoding either human L1 or the empty vector (mock) using Lipofectamine 2000 (Invitrogen) according to the manufacturer's instructions. The pcDNA3.1 plasmid containing the human L1 cDNA was kindly provided by Susan Kenwrick (Cambridge Institute for Medical Research, Cambridge, UK). Electrophysiological recordings were carried out 48–72 h after transfection. To identify transfected neurons, a co-transfection with a second plasmid containing the Tomato fluorescent protein reporter (Clontech) was used.

### MEA recordings and analysis of neuronal network firing activity

MEA recordings and analysis were performed as previously described (Chiappalone et al., 2009). Spikes representing spontaneous action potentials were detected by using a voltage-threshold-based algorithm run over 200 Hz high-pass-filtered traces; the voltage threshold was six-fold the standard deviation of the noise, and the refractory period was set to 2 ms. Groups of spikes occurring at a very high frequency (>10 Hz), defined as 'bursts', were identified according to the following criteria: 100 ms maximum inter-spike interval to include a spike in a burst, 10 ms minimum burst duration and a minimum of 5 spikes per burst. The following parameters were calculated: (1) the mean firing rate over a time window of 10 min; (2) the bursts per minute over a time window of 10 min; (3) the intra-burst frequency rate of spikes occurring within a burst; (4) the percentage spikes in the burst (the fraction of spikes occurring within bursts with respect to the total amount of spikes); and (5) burst duration.

### Patch-clamp recordings from dissociated cultured hippocampal neurons and acute hippocampal slices

Patch-clamp recordings were performed on cultured pyramidal neurons as previously described (Valente et al., 2012). Cultured pyramidal neurons were morphologically identified by their teardrop-shaped somata and characteristic apical dendrite after 12–16 div (Watt et al., 2000; Pratt et al., 2003). After recordings, pyramidal neurons were confirmed to be negative for GABA by immunocytochemistry (rabbit anti-GABA; 1:1000, Sigma-Aldrich, #A2052).

Current-clamp recordings of firing activity were performed in a standard external solution containing (in mM): 140 NaCl, 2 $CaCl_2$, 1 $MgCl_2$, 4 KCl, 10 glucose, 10 HEPES (pH 7.3 with NaOH). D-(-)-2-amino-5-phosphonopentanoic acid (D-AP5; 50 µM), 6-cyano-7-nitroquinoxaline-2,3-dione (CNQX; 10 µM) and bicuculline methiodide (30 µM) were added to the external solution on the day for blocking of NMDA, non-NMDA and $GABA_A$ receptors, respectively. The internal solution for action potential recordings contained (in mM): 126K gluconate, 4 NaCl, 1 $MgSO_4$, 0.02 $CaCl_2$, 0.1 BAPTA, 15 glucose, 5 HEPES, 3 ATP, 0.1 GTP (pH 7.2 with KOH). Unless otherwise indicated, −60 mV was the $V_h$ used for recording action potentials in the current-clamp configuration.

Voltage-clamp recordings of $Na^+$ currents were performed in standard extracellular solution containing (in mM): 120 NaCl, 4 KCl, 20 TEA-Cl, 10 HEPES, 2 $CaCl_2$, 1 $MgCl_2$, 10 glucose (pH 7.4 with NaOH). On the day of the experiment, D-AP5 (50 µM), CNQX (10 µM), bicuculline methiodide (30 µM) and $CdCl_2$ (100 µM) were added to the extracellular solution. The recording pipette solution contained (in mM): 100 CsMeS, 20 CsCl, 10 HEPES, 2 $MgCl_2$, 5 EGTA, 4 ATP, 15 phosphocreatine (pH 7.2 with CsOH). In all voltage-clamp experiments, the $V_h$ was set at −70 mV (Neher, 1992; Fricker et al., 1999). Patch-clamp recordings were performed on acute hippocampal slices as previously described (Farisello et al., 2013).

### Analysis of electrophysiological recordings from dissociated cultured hippocampal neurons and hippocampal slices

Firing activity was considered for analysis only from those cells with resting membrane potentials were between −57 and −64 mV. Action potential firing was induced by injecting 10 pA current steps of 1 s ($V_h$=−60 mV). Alternatively, action potential activity was studied by injecting a moderate depolarizing current to move the $V_h$ from the resting voltage ($V_{rest}$) to −50 mV for CA1 pyramidal neurons in slices and to −40 mV for dissociated excitatory neurons. At this voltage, pyramidal cells exhibit spontaneous firing activity that was recorded for 3–4 min. Firing frequency (F-freq) was calculated as the ratio of the number of action potentials evoked by current injection to the time interval between the first and the last evoked action potential. Instantaneous firing frequency was calculated as the reciprocal of the interspike interval between the first two action potentials evoked at the maximal value of injected current (160 pA).

The plot of the time-derivative of voltage ($dV/dt$) versus voltage, called the phase-plane plot, was obtained starting from the first action potential elicited by the minimal current injection. The voltage threshold was defined as the first voltage value at which $dV/dt$ exceeded 4 mV/ms. The rheobase was calculated as the minimum depolarizing current needed to elicit at least one action potential. The slopes of phase-plots at the action potential threshold (Naundorf et al., 2006; Shu et al., 2007) were calculated using linear regression of the first 10 data points of the rising phase with a $y$-value >4 mV/ms. The data were analyzed using pClamp (Molecular Devices) and Minianalysis (Synaptosoft, Inc.) software.

### Immunocytochemistry

Immunocytochemistry of cultured hippocampal neurons was performed as previously described (Piccini et al., 2015). For evaluation of the axonal length, cells were fixed after 2 and 4 div and probed with rabbit anti-βIII tubulin (1:1000, Sigma-Aldrich, #T2200) and mouse antibody against the pan-axonal neurofilament marker SMI-312 (1:300, Covance, #SMI-312R). For morphological identification of the AIS, cells were fixed at 14 div and probed with mouse antibodies against all isoforms of Nav1 ($PanNa_v$, 1:100, Sigma-Aldrich, #S8809) and ankyrinG (1:300, Santa Cruz Biotechnology). To quantify the immunofluorescence intensity at the AIS, images of cultured neurons were acquired with a Leica SP5 confocal microscope using a 63× objective and 1024×1024 pixels (1pixel=0.24 µm) in $z$-stack with 0.5 µm steps. To analyze stack images, a MATLAB script freely available at www.mathworks.com/matlabcentral/fileexchange/28181-ais-quantification was used as previously described (Grubb and Burrone, 2010). Briefly, a line profile was drawn along the fluorescently labeled AIS from the soma through and 5 µm past the AIS. Pixel fluorescence intensity values were averaged over a 3×3 pixel square centered on an arbitrarily drawn line, which was then smoothened using a 40-point sliding mean and normalized between 1 and 0 (maximum and minimum fluorescence intensity). The maximum position of the AIS was determined where the smoothed and normalized profile of fluorescence intensity reached its peak. The beginning and the end positions of the AIS were the proximal and distal sites, respectively, at which the profile dipped to 33% of its peak. The distance of the start, maximum and end positions

of the AIS from the soma were measured, by transmitted light, as the distance from the point where the neuronal process forming the axon had a diameter lower than 2 µm.

### Biochemistry

Immunoblotting with homogenates of cultured cortical neurons (14–16 div) or cortices (18–21-day-old mice) was carried out by standard methods. Biotinylation assays in cultured cortical neurons (14–16 div) were performed as previously described (Ferguson et al., 2009). The following primary antibodies were used: mouse anti-PanNa$_v$ (Sigma-Aldrich, #S8809, 1:1000), mouse anti-actin (Sigma-Aldrich, 1:5000), goat anti-L1 (Santa Cruz Biotechnology, #sc-1508, 1:200), rabbit anti-ankyrinG (Santa Cruz Biotechnology, #sc-28561, 1:500), rabbit anti-ankyrinB (Santa Cruz Biotechnology, #sc-28560, 1:1000), rabbit anti-p44/42 MAPK (ERK1/2; Cell Signaling, #4695, 1:5000), rabbit anti-phosphorylated-p44/42 MAPK (phospho-ERK1/2, Thr$^{202}$/Tyr$^{204}$; Cell Signaling, #4377, 1:1000) and mouse anti-Na/K ATPase α (Millipore, #05-369, 1:2000).

For immunoprecipitation, 10 µg of either anti-L1 antibodies or goat control IgGs (Sigma-Aldrich) were pre-coated with Protein-G–Sepharose (GE Healthcare) overnight and incubated with total mouse brain lysate in immunoprecipitation buffer (in mM: 150 NaCl, 50 Tris-HCl pH 7.4, 2 EDTA, 1% Triton X-100). After extensive washes in immunoprecipitation buffer and detergent-free immunoprecipitation buffer, samples were resolved by SDS-PAGE and subjected to immunoblotting with anti-L1 and anti-ankyrinG antibodies.

### Real-time quantitative PCR

RNA was extracted from cortices of 18-day-old mice with QIAzol reagent and purified on RNeasy spin columns (Qiagen). Reverse transcription was performed as previously described (Pozzi et al., 2013). Gene expression data were normalized to GAPDH (glyceraldehyde-3-phosphate dehydrogenase) and PPIA (peptidylprolyl isomeraseA) by the multiple internal control gene method (Vandesompele et al., 2002) with the GeNorm algorithm available in the qBasePlus software (Biogazelle, Ghent, Belgium).

Primers sequences were: GAPDH-F, 5′-GAACATCATCCCTGCATCCA-3′; GAPDH-R, 5′-CCAGTGAGCTTCCCGTTCA-3′; PPIA-F, 5′-CACTGTCGCTTTTCGCCGCTTG-3′; PPIA-R, 5′-TTTCTGCTGTCTTTGGAACTTTGTCTGC-3′; AnkG-F, 5′-ACTCGGTCCTTACCACCACTGT-3′; AnkG-R, 5′-TCTGGTACTTGTCTTCTGGCTGGA-3′; Nav1.1-F, 5′-GTGTGGATGCTGCCAATGC-3′; Nav1.1-R, 5′-CCTTGACTTAGCCACTGACCTATG-3′; Nav1.2-F, 5′-GGCTCTGCTGTCATTGTTGGTA-3′; Nav1.2-R, 5′-GAAGGCTAGGTGAGTACATCCC-3′; Nav1.6-F, 5′-CCATAAACGCTGCTATTCTGAGAG-3′; and Nav1.6-R, 5′-CCTGCTGTCCTGGTGATGA-3′.

### Statistical analysis

Statistical analyses are detailed in the figure legends. Data are given as means±s.e.m. for *n* sample size. Normal distribution of data was assessed using a Kolmogorov–Smirnov test. To compare two normally distributed sample groups, the Student's unpaired two-tailed *t*-test was used. For two sample groups that were not normally distributed, the non-parametric Mann–Whitney's U test was used. More than two normally distributed sample groups were compared by one-way ANOVA, followed by the Fisher's-test. Alpha-levels for all tests were 0.5% (95% confidence intervals). Statistical analysis was carried out by using OriginPro8 (OriginLab Corp., USA).

#### Acknowledgements

We wish to thank Jacopo Meldolesi for helpful discussions and Silvia Casagrande for precious help with cell cultures.

#### Competing interests

The authors declare no competing or financial interests.

#### Author contributions

P.B. and P.V. designed the study, performed experiments, analyzed data and wrote the paper. G.L., L.M. and S.G. performed experiments, analyzed data and co-wrote the paper. F. Benfenati and M.S. critically discussed the data and co-wrote the paper. F. Bosco and A.C. performed experiments and analyzed data. P.L. and E.F. performed MEA experiments.

#### Funding

This study was supported by research grants from the Italian Ministry of University and Research (Progetti di Rilevante Interesse Nazionale to F.B.); the Italian Ministry of Health, Bando Giovani Ricercatori 2009 [grant number GR-2009-1473821 to P.B.]; Futuro in Ricerca FIRB 2010 (to S.G.); Fondazione Cariplo [grant number 2013-0735 to F.B.]; and the EU Seventh Framework Programme Integrating Project 'Desire' [grant number 602531 to F.B.]. The support of Fondazione Telethon [grant number GGP13033 to F.B.] is also acknowledged.

#### References

**Appel, F., Holm, J., Conscience, J. F. and Schachner, M.** (1993). Several extracellular domains of the neural cell adhesion molecule L1 are involved in neurite outgrowth and cell body adhesion. *J. Neurosci.* **13**, 4764-4775.

**Barry, J., Gu, Y., Jukkola, P., O'Neill, B., Gu, H., Mohler, P. J., Rajamani, K. T. and Gu, C.** (2014). Ankyrin-G directly binds to kinesin-1 to transport voltage-gated Na+ channels into axons. *Dev. Cell* **28**, 117-131.

**Bean, B. P.** (2007). The action potential in mammalian central neurons. *Nat. Rev. Neurosci.* **8**, 451-465.

**Beaudoin, G. M., III, Lee, S.-H., Singh, D., Yuan, Y., Ng, Y.-G., Reichardt, L. F. and Arikkath, J.** (2012). Culturing pyramidal neurons from the early postnatal mouse hippocampus and cortex. *Nat. Protoc.* **7**, 1741-1754.

**Becker, C. G., Lieberoth, B. C., Morellini, F., Feldner, J., Becker, T. and Schachner, M.** (2004). L1.1 is involved in spinal cord regeneration in adult zebrafish. *J. Neurosci.* **24**, 7837-7842.

**Bennett, V. and Baines, A. J.** (2001). Spectrin and ankyrin-based pathways: metazoan inventions for integrating cells into tissues. *Physiol. Rev.* **81**, 1353-1392.

**Bennett, V. and Chen, L.** (2001). Ankyrins and cellular targeting of diverse membrane proteins to physiological sites. *Curr. Opin. Cell Biol.* **13**, 61-67.

**Boiko, T., Vakulenko, M., Ewers, H., Yap, C. C., Norden, C. and Winckler, B.** (2007). Ankyrin-dependent and -independent mechanisms orchestrate axonal compartmentalization of L1 family members neurofascin and L1/neuron-glia cell adhesion molecule. *J. Neurosci.* **27**, 590-603.

**Boyd, E., Schwartz, C. E., Schroer, R. J., May, M. M., Shapiro, S. D., Arena, J. F., Lubs, H. A. and Stevenson, R. E.** (1993). Agenesis of the corpus callosum associated with MASA syndrome. *Clin. Dysmorphol.* **2**, 332-341.

**Cavallaro, U. and Dejana, E.** (2011). Adhesion molecule signalling: not always a sticky business. *Nat. Rev. Mol. Cell Biol.* **12**, 189-197.

**Chan, W., Kordeli, E. and Bennett, V.** (1993). 440-kD ankyrinB: structure of the major developmentally regulated domain and selective localization in unmyelinated axons. *J. Cell Biol.* **123**, 1463-1473.

**Chiappalone, M., Casagrande, S., Tedesco, M., Valtorta, F., Baldelli, P., Martinoia, S. and Benfenati, F.** (2009). Opposite changes in glutamatergic and GABAergic transmission underlie the diffuse hyperexcitability of synapsin I-deficient cortical networks. *Cereb. Cortex* **19**, 1422-1439.

**Chung, R. S., Vickers, J. C., Chuah, M. I. and West, A. K.** (2003). Metallothionein-IIA promotes initial neurite elongation and postinjury reactive neurite growth and facilitates healing after focal cortical brain injury. *J. Neurosci.* **23**, 3336-3342.

**Cohen, N. R., Taylor, J. S. H., Scott, L. B., Guillery, R. W., Soriano, P. and Furley, A. J. W.** (1998). Errors in corticospinal axon guidance in mice lacking the neural cell adhesion molecule L1. *Curr. Biol.* **8**, 26-33.

**Colbert, C. M. and Johnston, D.** (1996). Axonal action-potential initiation and Na+ channel densities in the soma and axon initial segment of subicular pyramidal neurons. *J. Neurosci.* **16**, 6676-6686.

**Colombo, F., Racchetti, G. and Meldolesi, J.** (2014). Neurite outgrowth induced by NGF or L1CAM via activation of the TrkA receptor is sustained also by the exocytosis of enlargeosomes. *Proc. Natl. Acad. Sci. USA* **111**, 16943-16948.

**Dahme, M., Bartsch, U., Martini, R., Anliker, B., Schachner, M. and Mantei, N.** (1997). Disruption of the mouse L1 gene leads to malformations of the nervous system. *Nat. Genet.* **17**, 346-349.

**Davis, J. Q. and Bennett, V.** (1994). Ankyrin binding activity shared by the neurofascin/L1/NrCAM family of nervous system cell adhesion molecules. *J. Biol. Chem.* **269**, 27163-27166.

**Demyanenko, G. P., Tsai, A. Y. and Maness, P. F.** (1999). Abnormalities in neuronal process extension, hippocampal development, and the ventricular system of L1 knockout mice. *J. Neurosci.* **19**, 4907-4920.

**Dityatev, A. and Schachner, M.** (2003). Extracellular matrix molecules and synaptic plasticity. *Nat. Rev. Neurosci.* **4**, 456-468.

**Dityatev, A., Dityateva, G. and Schachner, M.** (2000). Synaptic strength as a function of post- versus presynaptic expression of the neural cell adhesion molecule NCAM. *Neuron* **26**, 207-217.

**Dityatev, A., Schachner, M. and Sonderegger, P.** (2010). The dual role of the extracellular matrix in synaptic plasticity and homeostasis. *Nat. Rev. Neurosci.* **11**, 735-746.

**Djabali, M., Mattei, M.-G., Nguyen, C., Roux, D., Demengeot, J., Denizot, F., Moos, M., Schachner, M., Goridis, C. and Jordan, B. R.** (1990). The gene encoding L1, a neural adhesion molecule of the immunoglobulin family, is located on the X chromosome in mouse and man. *Genomics* **7**, 587-593.

**Djogo, N., Jakovcevski, I., Müller, C., Lee, H. J., Xu, J.-C., Jakovcevski, M., Kugler, S., Loers, G. and Schachner, M.** (2013). Adhesion molecule L1 binds to amyloid beta and reduces Alzheimer's disease pathology in mice. *Neurobiol. Dis.* **56**, 104-115.

**Enneking, E.-M., Kudumala, S. R., Moreno, E., Stephan, R., Boerner, J., Godenschwege, T. A. and Pielage, J.** (2013). Transsynaptic coordination of synaptic growth, function, and stability by the L1-type CAM Neuroglian. *PLoS Biol.* **11**, e1001537.

**Farisello, P., Boido, D., Nieus, T., Medrihan, L., Cesca, F., Valtorta, F., Baldelli, P. and Benfenati, F.** (2013). Synaptic and extrasynaptic origin of the excitation/inhibition imbalance in the hippocampus of synapsin I/II/III knockout mice. *Cereb. Cortex* **23**, 581-593.

**Fassio, A., Patry, L., Congia, S., Onofri, F., Piton, A., Gauthier, J., Pozzi, D., Messa, M., Defranchi, E., Fadda, M. et al.** (2011). SYN1 loss-of-function mutations in autism and partial epilepsy cause impaired synaptic function. *Hum. Mol. Genet.* **20**, 2297-2307.

**Ferguson, S., Raimondi, A., Paradise, S., Shen, H., Mesaki, K., Ferguson, A., Destaing, O., Ko, G., Takasaki, J., Cremona, O. et al.** (2009). Coordinated actions of actin and BAR proteins upstream of dynamin at endocytic clathrin-coated pits. *Dev. Cell* **17**, 811-822.

**Fricker, D., Verheugen, J. A. H. and Miles, R.** (1999). Cell-attached measurements of the firing threshold of rat hippocampal neurones. *J. Physiol.* **517**, 791-804.

**Garrido, J. J., Giraud, P., Carlier, E., Fernandes, F., Moussif, A., Fache, M.-P., Debanne, D. and Dargent, B.** (2003). A targeting motif involved in sodium channel clustering at the axonal initial segment. *Science* **300**, 2091-2094.

**Gasser, A., Ho, T. S.-Y., Cheng, X., Chang, K.-J., Waxman, S. G., Rasband, M. N. and Dib-Hajj, S. D.** (2012). An ankyrinG-binding motif is necessary and sufficient for targeting Nav1.6 sodium channels to axon initial segments and nodes of Ranvier. *J. Neurosci.* **32**, 7232-7243.

**Goulding, M.** (2004). How early is firing required for wiring? *Neuron* **43**, 601-603.

**Grubb, M. S. and Burrone, J.** (2010). Activity-dependent relocation of the axon initial segment fine-tunes neuronal excitability. *Nature* **465**, 1070-1074.

**Guseva, D., Angelov, D. N., Irintchev, A. and Schachner, M.** (2009). Ablation of adhesion molecule L1 in mice favours Schwann cell proliferation and functional recovery after peripheral nerve injury. *Brain* **132**, 2180-2195.

**Hortsch, M., Nagaraj, K. and Godenschwege, T. A.** (2009). The interaction between L1-type proteins and ankyrins - a master switch for L1-type CAM function. *Cell. Mol. Biol. Lett.* **14**, 57-69.

**Huber, K. M., Gallagher, S. M., Warren, S. T. and Bear, M. F.** (2002). Altered synaptic plasticity in a mouse model of fragile X mental retardation. *Proc. Natl. Acad. Sci. USA* **99**, 7746-7750.

**Isom, L. L.** (2002). The role of sodium channels in cell adhesion. *Front. Biosci.* **7**, 12-23.

**Isom, L. L. and Catterall, W. A.** (1996). Na+ channel subunits and Ig domains. *Nature* **383**, 307-308.

**Kamiguchi, H., Hlavin, M. L. and Lemmon, V.** (1998). Role of L1 in neural development: what the knockouts tell us. *Mol. Cell. Neurosci.* **12**, 48-55.

**Kenwrick, S. and Doherty, P.** (1998). Neural cell adhesion molecule L1: relating disease to function. *Bioessays* **20**, 668-675.

**Kenwrick, S., Ionasescu, V., Ionasescu, G., Searby, C., King, A., Dubowitz, M. and Davies, K. E.** (1986). Linkage studies of X-linked recessive spastic paraplegia using DNA probes. *Hum. Genet.* **73**, 264-266.

**Kole, M. H. P. and Stuart, G. J.** (2008). Is action potential threshold lowest in the axon? *Nat. Neurosci.* **11**, 1253-1255.

**Kole, M. H. P., Ilschner, S. U., Kampa, B. M., Williams, S. R., Ruben, P. C. and Stuart, G. J.** (2008). Action potential generation requires a high sodium channel density in the axon initial segment. *Nat. Neurosci.* **11**, 178-186.

**Kuba, H., Oichi, Y. and Ohmori, H.** (2010). Presynaptic activity regulates Na(+) channel distribution at the axon initial segment. *Nature* **465**, 1075-1078.

**Kunz, S., Ziegler, U., Kunz, B. and Sonderegger, P.** (1996). Intracellular signaling is changed after clustering of the neural cell adhesion molecules axonin-1 and NgCAM during neurite fasciculation. *J. Cell Biol.* **135**, 253-267.

**Law, J. W., Lee, A. Y., Sun, M., Nikonenko, A. G., Chung, S. K., Dityatev, A., Schachner, M. and Morellini, F.** (2003). Decreased anxiety, altered place learning, and increased CA1 basal excitatory synaptic transmission in mice with conditional ablation of the neural cell adhesion molecule L1. *J. Neurosci.* **23**, 10419-10432.

**Lemaillet, G., Walker, B. and Lambert, S.** (2003). Identification of a conserved ankyrin-binding motif in the family of sodium channel alpha subunits. *J. Biol. Chem.* **278**, 27333-27339.

**Lindner, J., Rathjen, F. G. and Schachner, M.** (1983). L1 mono- and polyclonal antibodies modify cell migration in early postnatal mouse cerebellum. *Nature* **305**, 427-430.

**Lüthl, A., Laurent, J.-P., Figurov, A., Muller, D. and Schachner, M.** (1994). Hippocampal long-term potentiation and neural cell adhesion molecules L1 and NCAM. *Nature* **372**, 777-779.

**Lutz, D., Wolters-Eisfeld, G., Joshi, G., Djogo, N., Jakovcevski, I., Schachner, M. and Kleene, R.** (2012). Generation and nuclear translocation of sumoylated transmembrane fragment of cell adhesion molecule L1. *J. Biol. Chem.* **287**, 17161-17175.

**Malhotra, J. D., Koopmann, M. C., Kazen-Gillespie, K. A., Fettman, N., Hortsch, M. and Isom, L. L.** (2002). Structural requirements for interaction of sodium channel beta 1 subunits with ankyrin. *J. Biol. Chem.* **277**, 26681-26688.

**Maness, P. F. and Schachner, M.** (2007). Neural recognition molecules of the immunoglobulin superfamily: signaling transducers of axon guidance and neuronal migration. *Nat. Neurosci.* **10**, 19-26.

**McCormick, D. A., Shu, Y. and Yu, Y.** (2007). Neurophysiology: Hodgkin and Huxley model — still standing? *Nature* **445**, E1-E2; discussion E2-3.

**Milescu, L. S., Bean, B. P. and Smith, J. C.** (2010). Isolation of somatic Na+ currents by selective inactivation of axonal channels with a voltage prepulse. *J. Neurosci.* **30**, 7740-7748.

**Naundorf, B., Wolf, F. and Volgushev, M.** (2006). Unique features of action potential initiation in cortical neurons. *Nature* **440**, 1060-1063.

**Neher, E.** (1992). Correction for liquid junction potentials in patch clamp experiments. *Methods Enzymol.* **207**, 123-131.

**Nishimura, K., Yoshihara, F., Tojima, T., Ooashi, N., Yoon, W., Mikoshiba, K., Bennett, V. and Kamiguchi, H.** (2003). L1-dependent neuritogenesis involves ankyrin B that mediates L1-CAM coupling with retrograde actin flow. *J. Cell Biol.* **163**, 1077-1088.

**Palmer, L. M. and Stuart, G. J.** (2006). Site of action potential initiation in layer 5 pyramidal neurons. *J. Neurosci.* **26**, 1854-1863.

**Pan, Z., Kao, T., Horvath, Z., Lemos, J., Sul, J.-Y., Cranstoun, S. D., Bennett, V., Scherer, S. S. and Cooper, E. C.** (2006). A common ankyrin-G-based mechanism retains KCNQ and NaV channels at electrically active domains of the axon. *J. Neurosci.* **26**, 2599-2613.

**Piccini, A., Perlini, L. E., Cancedda, L., Benfenati, F. and Giovedi, S.** (2015). Phosphorylation by PKA and Cdk5 mediates the early effects of synapsin III in neuronal morphological maturation. *J. Neurosci.* **35**, 13148-13159.

**Poplawsky, J. and Dierolf, V.** (2012). High-resolution confocal microscopy with simultaneous electron and laser beam irradiation. *Microsc. Microanal.* **18**, 1263-1269.

**Pozzi, D., Lignani, G., Ferrea, E., Contestabile, A., Paonessa, F., D'alessandro, R., Lippiello, P., Boido, D., Fassio, A., Meldolesi, J. et al.** (2013). REST/NRSF-mediated intrinsic homeostasis protects neuronal networks from hyperexcitability. *EMBO J.* **32**, 2994-3007.

**Pratt, K. G., Watt, A. J., Griffith, L. C., Nelson, S. B. and Turrigiano, G. G.** (2003). Activity-dependent remodeling of presynaptic inputs by postsynaptic expression of activated CaMKII. *Neuron* **39**, 269-281.

**Rasband, M. N.** (2008). Na+ channels get anchored…with a little help. *J. Cell Biol.* **183**, 975-977.

**Riedle, S., Kiefel, H., Gast, D., Bondong, S., Wolterink, S., Gutwein, P. and Altevogt, P.** (2009). Nuclear translocation and signalling of L1-CAM in human carcinoma cells requires ADAM10 and presenilin/gamma-secretase activity. *Biochem. J.* **420**, 391-402.

**Rolf, B., Kutsche, M. and Bartsch, U.** (2001). Severe hydrocephalus in L1-deficient mice. *Brain Res.* **891**, 247-252.

**Roonprapunt, C., Huang, W., Grill, R., Friedlander, D., Grumet, M., Chen, S., Schachner, M. and Young, W.** (2003). Soluble cell adhesion molecule L1-Fc promotes locomotor recovery in rats after spinal cord injury. *J. Neurotrauma* **20**, 871-882.

**Saghatelyan, A. K., Nikonenko, A. G., Sun, M., Rolf, B., Putthoff, P., Kutsche, M., Bartsch, U., Dityatev, A. and Schachner, M.** (2004). Reduced GABAergic transmission and number of hippocampal perisomatic inhibitory synapses in juvenile mice deficient in the neural cell adhesion molecule L1. *Mol. Cell. Neurosci.* **26**, 191-203.

**Schachner, M.** (1997). Neural recognition molecules and synaptic plasticity. *Curr. Opin. Cell Biol.* **9**, 627-634.

**Schaefer, A. W., Kamiguchi, H., Wong, E. V., Beach, C. M., Landreth, G. and Lemmon, V.** (1999). Activation of the MAPK signal cascade by the neural cell adhesion molecule L1 requires L1 internalization. *J. Biol. Chem.* **274**, 37965-37973.

**Scotland, P., Zhou, D., Benveniste, H. and Bennett, V.** (1998). Nervous system defects of Ankyrin B (–/–) mice suggest functional overlap between the cell adhesion molecule L1 and 440-kD Ankyrin B in premyelinated axons. *J. Cell Biol.* **143**, 1305-1315.

**Seilheimer, B., Persohn, E. and Schachner, M.** (1989). Neural cell adhesion molecule expression is regulated by Schwann cell-neuron interactions in culture. *J. Cell Biol.* **108**, 1909-1915.

**Shepherd, G. M. G. and Katz, D. M.** (2011). Synaptic microcircuit dysfunction in genetic models of neurodevelopmental disorders: focus on Mecp2 and Met. *Curr. Opin. Neurobiol.* **21**, 827-833.

**Shu, Y., Duque, A., Yu, Y., Haider, B. and McCormick, D. A.** (2007). Properties of action-potential initiation in neocortical pyramidal cells: evidence from whole cell axon recordings. *J. Neurophysiol.* **97**, 746-760.

**Silletti, S., Yebra, M., Perez, B., Cirulli, V., Mcmahon, M. and Montgomery, A. M. P.** (2004). Extracellular signal-regulated kinase (ERK)-dependent gene expression contributes to L1 cell adhesion molecule-dependent motility and invasion. *J. Biol. Chem.* **279**, 28880-28888.

**Stuart, G., Schiller, J. and Sakmann, B.** (1997). Action potential initiation and propagation in rat neocortical pyramidal neurons. *J. Physiol.* **505**, 617-632.



Journal of Cell Science

**Vacher, H., Mohapatra, D. P. and Trimmer, J. S.** (2008). Localization and targeting of voltage-dependent ion channels in mammalian central neurons. *Physiol. Rev.* **88**, 1407-1447.

**Valente, P., Casagrande, S., Nieus, T., Verstegen, A. M. J., Valtorta, F., Benfenati, F. and Baldelli, P.** (2012). Site-specific synapsin I phosphorylation participates in the expression of post-tetanic potentiation and its enhancement by BDNF. *J. Neurosci.* **32**, 5868-5879.

**Van Camp, G., Vits, L., Coucke, P., Lyonnet, S., Schrander-Stumpel, C., Darby, J., Holden, J., Munnich, A. and Willems, P. J.** (1993). A duplication in the L1CAM gene associated with X–linked hydrocephalus. *Nat. Genet.* **4**, 421-425.

**Vandesompele, J., De Preter, K., Pattyn, F., Poppe, B., Van Roy, N., De Paepe, A. and Speleman, F.** (2002). Accurate normalization of real-time quantitative RT-PCR data by geometric averaging of multiple internal control genes. *Genome Biol.* **3**, RESEARCH0034.

**Watt, A. J., Van Rossum, M. C. W., MacLeod, K. M., Nelson, S. B. and Turrigiano, G. G.** (2000). Activity coregulates quantal AMPA and NMDA currents at neocortical synapses. *Neuron* **26**, 659-670.

**Weller, S. and Gärtner, J.** (2001). Genetic and clinical aspects of X-linked hydrocephalus (L1 disease): Mutations in the L1CAM gene. *Hum. Mutat.* **18**, 1-12.

**Wood, P. M., Schachner, M. and Bunge, R. P.** (1990). Inhibition of Schwann cell myelination in vitro by antibody to the L1 adhesion molecule. *J. Neurosci.* **10**, 3635-3645.

**Yanagita, T., Kobayashi, H., Uezono, Y., Yokoo, H., Sugano, T., Saitoh, T., Minami, S.-I., Shiraishi, S. and Wada, A.** (2003). Destabilization of Na(v)1.7 sodium channel alpha-subunit mRNA by constitutive phosphorylation of extracellular signal-regulated kinase: negative regulation of steady-state level of cell surface functional sodium channels in adrenal chromaffin cells. *Mol. Pharmacol.* **63**, 1125-1136.

**Yu, Y., Shu, Y. and McCormick, D. A.** (2008). Cortical action potential backpropagation explains spike threshold variability and rapid-onset kinetics. *J. Neurosci.* **28**, 7260-7272.

**Zhou, D., Lambert, S., Malen, P. L., Carpenter, S., Boland, L. M. and Bennett, V.** (1998). Ankyrin G is required for clustering of voltage-gated Na channels at axon initial segments and for normal action potential firing. *J. Cell Biol.* **143**, 1295-1304.